

# Efficient generation of tunable photon pairs at 0.8 and 1.6 $\mu\text{m}$

Elliott J. Mason, Marius A. Albota, Friedrich König, and Franco N. C. Wong

Research Laboratory of Electronics, Massachusetts Institute of Technology, Cambridge, Massachusetts 02139

Received July 9, 2002

We demonstrate efficient generation of collinearly propagating, highly nondegenerate photon pairs in a periodically poled lithium niobate cw parametric downconverter with an inferred pair generation rate of  $1.4 \times 10^7/\text{s}/\text{mW}$  of pump power. Detection of an 800-nm signal photon triggers a thermoelectrically cooled 20%-efficient InGaAs avalanche photodiode for the detection of the 1600-nm conjugate idler photon. Using single-mode fibers as spatial mode filters, we obtain a signal-conditioned idler-detection probability of  $\sim 3.1\%$ . © 2002 Optical Society of America

OCIS codes: 270.0270, 030.5260, 190.4410, 270.5570.

Efficient generation of entangled photons is essential for realizing practical quantum information processing applications such as quantum cryptography and quantum teleportation. Entangled photons are routinely generated by spontaneous parametric downconversion (SPDC) in a nonlinear crystal.<sup>1</sup> More recently, nonlinear waveguides were used for photon pair generation with high efficiency<sup>2–4</sup> and better control of the spatial modes. So far, these entangled photon sources have large bandwidths. Recently, a narrowband application was suggested in a singlet-based quantum teleportation system<sup>5</sup> in which narrowband (tens of megahertz) polarization-entangled photons are needed for loading quantum memories that are composed of trapped Rb in optical cavities.<sup>6</sup> Such a narrowband source is most conveniently produced with a resonant cavity such as an optical parametric amplifier (OPA).<sup>7,8</sup> In addition to being narrowband, the OPA outputs have well-defined spatial modes that allow efficient coupling into trapped-Rb cavities. The requirements for efficient generation in an OPA and in SPDC are different. In an OPA, collinearly propagating signal and idler beams are necessary to minimize walk-off, and intracavity losses must be small compared with the cavity's output coupling. A desirable configuration consists of a long crystal with light propagation along one of its principal axes. In contrast, a nonlinear waveguide is an excellent choice for SPDC but is ill suited for intracavity use because of high waveguide propagation losses.

As a precursor to an OPA configuration, we have studied the generation of collinearly propagating tunable outputs at  $\sim 800$  and  $\sim 1600$  nm in a quasi-phase-matched periodically poled lithium niobate parametric downconverter. Unlike most other SPDC sources, our periodically poled lithium niobate source utilizes a long bulk crystal, which results in a small bandwidth, and the two output wavelengths are widely separated. The choice of wavelengths is designed for loading local Rb-based quantum memories at 795 nm and for low-loss fiber-optic transmission of the conjugate photons at  $\sim 1.6 \mu\text{m}$ . The 1600-nm photon can be upconverted via quantum frequency translation<sup>9</sup> for remote quantum memory loading. For the current work, we constructed a compact

all-solid-state InGaAs single-photon counter for detecting the 1.6- $\mu\text{m}$  photons.

We tested three fiber-pigtailed InGaAs avalanche photodiodes (APDs) from JDS Uniphase (EPM239BA) as passively quenched, gated single-photon counters.<sup>10–12</sup> Each APD was mounted in a small copper block that was attached to a four-stage thermoelectric cooler, which in turn was in contact with a brass heat sink. We placed this thermoelectric-cooled APD assembly in a sealed box mounted on top of four additional TE coolers for improved temperature control of the APD box. Using this all-solid-state cooling apparatus, we were able to adjust the APD temperature down to  $-60^\circ\text{C}$  without the use of liquid nitrogen. Typically we biased the APDs at 0.2–1.0 V below the breakdown voltage of the selected APD device, and we applied a gating pulse of 2–4 V to overbias the APDs for single-photon detection. The gate pulses had rise and fall times of 3–4 ns with subnanosecond timing jitters, and the adjustable pulse length was set at 20 ns. The avalanche output pulses were then amplified by 40 dB with resultant pulse amplitudes of 1–2 V and rise times of less than 2 ns.

In general, dark counts increase exponentially with increasing device temperatures, and hence a lower operating temperature is preferred. However, afterpulsing due to trapped charge carriers increases with lower temperatures and also with longer gate durations and higher gate repetition rates. We have found that at an operating temperature of  $-50^\circ\text{C}$  there was negligible afterpulsing for gating frequencies of 100 kHz or less, and the dark counts were low enough to yield a high signal-to-noise ratio (see Fig. 3, below). Figure 1

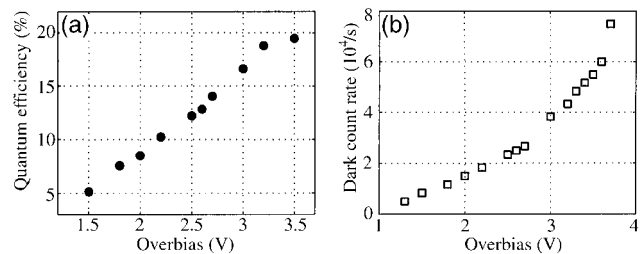


Fig. 1. (a) Quantum efficiency (filled circles) and (b) dark count rate (open squares) of an InGaAs APD with a 20-ns gate at  $-50^\circ\text{C}$  as a function of overbias voltage.

shows the quantum efficiencies (filled circles) and dark count rates (open squares) of one of the three APDs at an operating temperature of  $-50^\circ\text{C}$  as a function of the overbias voltage. We measured the quantum efficiency of the APD device with a  $1.56\text{-}\mu\text{m}$  fiber-pigtailed cw laser. The laser power was attenuated with variable fiber-optic attenuators to 0.13 photon per 20-ns gate ( $\sim 0.85\text{ pW}$ ), and the power was monitored with fiber-optic tap couplers and a high-accuracy optical powermeter with a large dynamic range. For our coincidence measurements, we chose the best of the three APDs and operated it at  $-50^\circ\text{C}$  with an overbias of 3.7 V. Under these operating conditions, we achieved a quantum efficiency of  $\sim 20\%$  with negligible afterpulses and a dark count probability of  $1.1 \times 10^{-3}$  per 20-ns gate.

We fabricated a 20-mm-long, 0.5-mm-thick periodically poled  $\text{LiNbO}_3$  (PPLN) crystal with a grating period of  $21.6\text{ }\mu\text{m}$  for type I third-order quasi-phase matching. The PPLN was antireflection coated on both facets at 800 and 1600 nm (with  $\sim 8\%$  reflection per surface at 532 nm) and was housed in a temperature-stabilized oven with a stability of  $\pm 0.1^\circ\text{C}$ . We first characterized the PPLN by performing difference frequency generation (DFG) with a strong pump at 532 nm and a weak tunable (1580–1610 nm) external-cavity diode laser. We also used a distributed feedback laser at 1559 nm to generate DFG light at 808 nm. We achieved tunable outputs by changing the oven temperature between 140 and  $185^\circ\text{C}$  with a measured tuning coefficient of  $\sim 1.3\text{ nm}/^\circ\text{C}$  for the 1600-nm light. At a fixed temperature the DFG bandwidth in the probe wavelength was  $1.26\text{ nm}$  ( $\sim 150\text{ GHz}$ ), in good agreement with the expected value for a 20-mm-long PPLN. From the DFG output powers we estimate that the effective nonlinear coefficient was  $3.8\text{ pm/V}$  for the third-order quasi-phase matching, which is lower than expected because of nonuniformity and the suboptimal duty cycle of the PPLN grating and also because of pump–probe mode mismatch.

For coincidence measurements, we set the PPLN oven at  $142^\circ\text{C}$ , which centered the signal and idler outputs at 808 and 1559 nm, respectively. The cw pump at 532 nm was focused at the center of the crystal with a waist of  $\sim 90\text{ }\mu\text{m}$ . The copolarized, collinearly propagating SPDC outputs were spatially separated with a prism at the Brewster angle for detection by a commercial Si single-photon counting module for the 808-nm signal photons and by the InGaAs APD single-photon counter for the 1559-nm idler photons. The single-photon counting module (Perkin-Elmer SPCM-AQR-14) had a quantum efficiency of  $\sim 54\%$  at 800 nm with a dark count rate below 100/s. We first measured the singles rate by collecting the freely propagating signal photons to obtain an inferred pair generation rate of  $1.4 \times 10^7/\text{s/mW}$  of pump power. The signal was also tuned to other wavelengths within the temperature tuning range, and we obtained similar singles rates. With the  $\sim 150\text{-GHz}$  signal bandwidth, the spectral brightness of the output was  $9 \times 10^4\text{ pairs/s/GHz/mW}$  of pump power, indicating that the long bulk PPLN crystal was very efficient

even though only third-order quasi-phase matching was used.

Spatial mode matching between the signal and idler is a problem with SPDC because of its spontaneous nature and hence its lack of spatial mode selection. Often an interference filter and a small aperture are used to select a narrow spectral width and a small number of spatial modes of a multimode field to yield high visibility in a Hong–Ou–Mandel interferometric measurement. Even SPDC in a waveguide does not necessarily eliminate the spatial mode-matching problem.<sup>4</sup> We took a different approach by coupling the SPDC outputs into single-mode fibers<sup>13</sup> without interference filters. By using a probe laser we measured a fiber coupling efficiency of a well-defined single transverse mode to be  $\sim 50\%$ . For the SPDC signal at 808 nm we measured a singles rate of  $3 \times 10^4/\text{s/mW}$  of pump power (typical pump powers of 1–2 mW were used). For a measured propagation efficiency of  $\sim 85\%$ , a Si detector efficiency of  $\sim 54\%$ , and a fiber coupling efficiency of  $\sim 50\%$ , we obtain an inferred generation rate of  $\sim 1.3 \times 10^5/\text{s/mW}$  for the single-mode signal photons, which is a factor of 100 smaller than that inferred from our multimode free-space detection rate. The challenge in our coincidence measurements was to match the single spatial modes of the highly nondegenerate signal and idler to their respective fibers.

Figure 2 shows the experimental setup for signal–idler coincidence measurements. The signal photon was coupled into an 800-nm single-mode optical fiber and was detected by the single-photon counting module, whose electrical output pulse was used to trigger the gate for the InGaAs detector. We set up the idler collection optics to select the spatial mode that was conjugate to the fiber-coupled signal mode. The idler mode was coupled into a 70-m-long 1550-nm single-mode fiber that provided a 345-ns time delay to allow the gating pulse to turn the InGaAs detector on shortly before the arrival of the idler photon. We limited the maximum trigger and detection rate to 10 kHz to avoid any afterpulsing effect. The outputs of the two detectors were recorded on a two-channel digitizing oscilloscope and stored for analysis. Figure 3 shows a histogram of the conditional detection probability,  $\eta_c$ , of a 1609-nm photon per detected 808-nm photon. The figure clearly shows that the dark count noise was quite small and the photon pairs were time coincident within a 4-ns window. The timing accuracy was limited by the 2-ns digitizing time

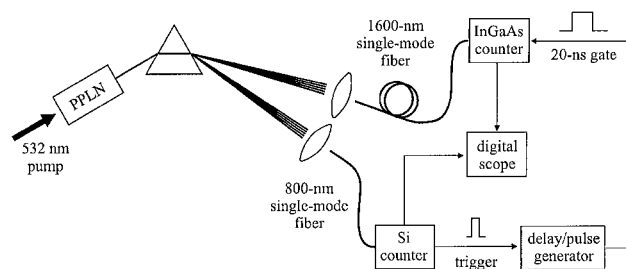


Fig. 2. Schematic of the experimental setup for coincidence measurements.

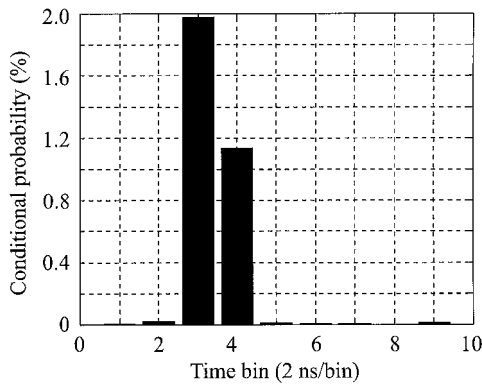


Fig. 3. Histograms of idler photon detection probability conditional on signal photon detection in 2-ns time bins over a 20-ns window. Accidental coincidences due to dark counts are barely noticeable outside the 4-ns coincidence window.

bin and the rise time of the InGaAs detector output pulse ( $\sim 2$  ns). We measured  $\eta_c \approx 3.1\%$ , limited by the InGaAs detector quantum efficiency of 20%, the propagation efficiency of 85%, and the single-mode fiber-coupling and the signal-idler mode-matching efficiency, which we infer to be  $\sim 18\%$ . This inferred coupling and mode-matching efficiency of 18% and our single-mode fiber-coupling efficiency of  $\sim 50\%$  of a probe laser suggest that the signal-idler mode matching was  $\sim 36\%$ .

In comparison, Banaszek *et al.*<sup>4</sup> reported a measured  $\eta_c$  of 18.5% for a waveguide SPDC and trigger-photon collection (at  $\sim 700$  nm) with a multimode fiber. If we adjust our results to assume a Si-type detection efficiency of  $\sim 70\%$  and no propagation losses, we infer  $\eta_c \approx 12.8\%$  for our single-mode fiber collection system. Kurtsiefer *et al.*<sup>13</sup> used single-mode fibers for collecting the degenerate outputs of a type II phase-matched SPDC and obtained an impressive  $\eta_c$  of 28.6%. Our lower  $\eta_c$  was probably a result of suboptimal collection optics, made more difficult by the widely different signal and idler wavelengths.

In summary, we have demonstrated an efficient cw source of highly nondegenerate photon pairs at

$\sim 800$  and  $\sim 1600$  nm that uses a long bulk PPLN crystal. Coincidence measurements were made with a home-built all-solid-state InGaAs single-photon counter for  $1.6\text{-}\mu\text{m}$  detection. Bidirectional pumping and judicious combining of the outputs<sup>7</sup> should allow us to efficiently generate nondegenerate polarization-entangled photons. Efforts are also under way to use the PPLN crystal in an OPA cavity configuration for generating high-flux narrowband photon pairs.

This work was supported by the U.S. Department of Defense Multidisciplinary University Research Initiative program administered by the U.S. Army Research Office under grant DAAD-19-00-1-0177 and by the National Reconnaissance Office. F. N. C. Wong thanks D. S. Bethune for fruitful discussions on detector bias circuitry.

## References

1. P. G. Kwiat, L. Mattle, H. Weinfurter, Z. Zeilinger, A. V. Sergienko, and Y. Shih, *Phys. Rev. Lett.* **75**, 4337 (1995).
2. S. Tanzilli, H. De Riedmatten, W. Tittel, H. Zbinden, P. Baldi, M. De Micheli, D. B. Ostrowsky, and N. Gisin, *Electron. Lett.* **37**, 26 (2001).
3. K. Sanaka, K. Kawahara, and T. Kuga, *Phys. Rev. Lett.* **86**, 5620 (2001).
4. K. Banaszek, A. B. U'Ren, and I. A. Walmsley, *Opt. Lett.* **26**, 1367 (2001).
5. J. H. Shapiro, *New J. Phys.* **4**, 47 (2002).
6. S. Lloyd, M. S. Shahriar, J. H. Shapiro, and P. R. Hemmer, *Phys. Rev. Lett.* **87**, 167903 (2001).
7. J. H. Shapiro and N. C. Wong, *J. Opt. B Quantum Semiclass. Opt.* **2**, L1 (2000).
8. Y. J. Lu and Z. Y. Ou, *Phys. Rev. A* **62**, 033804 (2000).
9. J. Huang and P. Kumar, *Phys. Rev. Lett.* **68**, 2153 (1992).
10. G. Ribordy, J.-D. Gautier, H. Zbinden, and N. Gisin, *Appl. Opt.* **37**, 2272 (1998).
11. D. S. Bethune and W. P. Risk, *IEEE J. Quantum Electron.* **36**, 340 (2000).
12. D. Stucki, G. Ribordy, A. Stefanov, H. Zbinden, J. G. Rarity, and T. Wall, *J. Mod. Opt.* **48**, 1967 (2001).
13. C. Kurtsiefer, M. Oberparleiter, and H. Weinfurter, *Phys. Rev. A* **64**, 023802 (2001).